

Supporting Information

for *Adv. Sci.*, DOI 10.1002/advs.202309155

Engineering of Aromatic Naphthalene and Solvent Molecules to Optimize Chemical
Prelithiation for Lithium-Ion Batteries

*Jagabandhu Patra, Shi-Xian Lu, Jui-Cheng Kao, Bing-Ruei Yu, Yu-Ting Chen, Yu-Sheng Su, Tzi-Yi
Wu, Dominic Bresser, Chien-Te Hsieh*, Yu-Chieh Lo* and Jeng-Kuei Chang**

Supporting Information

**Engineering of Aromatic Naphthalene and Solvent Molecules to Optimize
Chemical Prelithiation for Lithium-Ion Batteries**

*Jagabandhu Patra[#], Shi-Xian Lu[#], Jui-Cheng Kao, Bing-Ruei Yu, Yu-Ting Chen, Yu-Sheng Su,
Tzi-Yi Wu, Dominic Bresser, Chien-Te Hsieh*, Yu-Chieh Lo*, Jeng-Kuei Chang**

Table S1. Summary of charge-discharge performance of pristine, Li-Naph/G1, Li-2-M-Naph/G1, and Li-1-M-Naph/G1 HC electrodes.

| Specific current (mA g ⁻¹) | Pristine HC (mAh g ⁻¹) | Li-Naph/G1 (mAh g ⁻¹) | Li-2-M-Naph/G1 (mAh g ⁻¹) | Li-1-M-Naph/G1 (mAh g ⁻¹) |
|--|---------------------------------------|--------------------------------------|--|--|
| 50 | 320 | 321 | 320 | 322 |
| 100 | 268 | 281 | 290 | 300 |
| 200 | 230 | 248 | 260 | 270 |
| 500 | 190 | 210 | 222 | 233 |
| 1000 | 165 | 178 | 189 | 200 |
| 2000 | 144 | 154 | 163 | 177 |
| High rate retention (C ₅₀ /C ₂₀₀₀) | 45% | 48% | 51% | 55% |
| Capacity retained after 500 cycles | 80% | 81% | 84% | 90% |

Table S2. Summary of charge-discharge performance of Li-1-M-Naph/G1 Li-1-M-Naph/G2, and Li-1-M-Naph/G3 HC electrodes.

| Specific current (mA g ⁻¹) | Li-1-M-Naph/G1 (mAh g ⁻¹) | Li-1-M-Naph/G2 (mAh g ⁻¹) | Li-1-M-Naph/G3 (mAh g ⁻¹) |
|--|--|--|--|
| 50 | 322 | 320 | 321 |
| 100 | 300 | 269 | 258 |
| 200 | 270 | 230 | 210 |
| 500 | 233 | 178 | 156 |
| 1000 | 200 | 152 | 130 |
| 2000 | 177 | 125 | 109 |
| High rate retention (C ₅₀ /C ₂₀₀₀) | 55% | 39% | 34% |
| Capacity retained after 500 cycles | 90% | 80% | 78% |

Table S3. Summary of charge-discharge performance of various HC electrodes prelithiated using Li-1-M-Naph/G1 solution with different aging times.

| Specific current (mA g ⁻¹) | 2 h (mAh g ⁻¹) | 4 h (mAh g ⁻¹) | 6 h (mAh g ⁻¹) | 8 h (mAh g ⁻¹) | 10 h (mAh g ⁻¹) | 12 h (mAh g ⁻¹) |
|---|-------------------------------|-------------------------------|-------------------------------|-------------------------------|--------------------------------|--------------------------------|
| 50 | 320 | 320 | 321 | 321 | 322 | 321 |
| 100 | 273 | 281 | 290 | 297 | 300 | 299 |
| 200 | 235 | 244 | 255 | 262 | 270 | 267 |
| 500 | 200 | 208 | 219 | 225 | 233 | 230 |
| 1000 | 170 | 178 | 184 | 194 | 200 | 199 |
| 2000 | 147 | 153 | 163 | 170 | 177 | 176 |
| High rate retention (C ₅₀ /C ₂₀₀₀) | 46% | 48% | 51% | 53% | 55% | 55% |
| Cycle retention after 500 cycles (%) | 88% | 91% | 94% | 96% | 98% | 98% |

Table S4. Performance comparison of HC electrodes prelithiated using various approaches.

| Chemical prelithiation | | | | | | | | |
|--------------------------------------|-----------|------------------------|------------|--------------------|---------------------------|------------------------------|--|------------------|
| Anode material | Solvents | Aromatic compounds | ICE | Prelithiation time | Low rate capacity | High rate capacity | Cycling stability | Ref. |
| Hard carbon | THF | Biphenyl | ~106% | 30 second | ~288 Ah/g @30 mA/g | ~50 Ah/g @1500 mA/g | stable up to 100 cycles @300 mA/g | 1 |
| Hard carbon | G1 | Naphthalene | ~99.5% | 4 min | ~400 mAh/g @50 mA/g | ~195 mAh/g @4000 mA/g | stable up to 500 cycles @400 mA/g | 2 |
| Hard carbon | THF | 4,4-dimethyl biphenyl | ~100% | 1 min | ~275 mAh/g @15 mA/g | na | na | 3 |
| Hard carbon | THF | Biphenyl | 96% | 3 min | ~270 mAh/g @37.2mA/g | ~125 mAh/g @372mA/g | stable up to after 50 cycles @744 mA/g | 4 |
| Hard carbon | G1 | 1-M-Naphthalene | 98% | 1 min | 322 mAh/g @50 mA/g | ~177 mAh/g @2000 mA/g | 90% retention after 500 cycles @400 mA/g at 25 °C; 87% retention after 500 cycles @400 mA/g at 50 °C. | This work |
| Electrochemical prelithiation | | | | | | | | |
| Hard carbon | - | - | 65% | - | 250 mAh/g @50 mA/g | ~100 mAh/g @1200 mA/g | stable up to 400 cycles @30 mA/g | 5 |

Reference:

1. X. Zhang, H. Qu, W. Ji, D. Zheng, T. Ding, C. Abegglen, D. Qiu, D. Qu, *ACS Appl. Mater. Interfaces* **2020**, *12*, 11589.
2. Y. Shen, J. Qian, H. Yang, F. Zhong, X. Ai, *Small* **2020**, *16*, 1907602.
3. H. Yue, S. Zhang, T. Feng, C. Chen, H. Zhou, Z. Xu, M. Wu, *ACS Appl. Mater. Interfaces* **2021**, *13*, 45, 53996.
4. S. J. Hong, S. S. Kim, S. Nam, *Corros. Eng. Sci. Technol.* **2021**, *20*, 15.
5. M. Drews, J. Buttner, M. Bauer, J. Ahmed, R. Sahu, C. Scheu, S. Vierrath, A. Fischer, D. Biro, *ChemElectroChem* **2021**, *8*, 4750.

Table S5. Price comparison of various solvents and PAHs used for chemical prelithiation (according to <https://www.tcichemicals.com>).

| Solvents | Price (in USD) |
|-----------------------------------|-----------------------|
| Tetrahydropyran | 150/ 500 ml |
| 2-methyl-Tetrahydrofuran | 86/ 500 ml |
| ethylene glycol dimethyl ether | 59/ 500 ml |
| diethylene glycol dimethyl ether | 50/ 500 ml |
| triethylene glycol dimethyl ether | 68/ 500 ml |
| PAHs | Price (in USD) |
| 2-methylbiphenyl | 50/1 gm |
| 3,3',4,4'-Tetramethylbiphenyl | 63.25/ 1 gm* |
| 2-fluorobenzene | 16/ 25 gm |
| 4,4'-diethyl Biphenyl | 119/ 25 gm |
| 4-methylbiphenyl | 262/ 25 gm |
| 4,4'-di-tert-butylbiphenyl | 88/ 25 gm |
| 4,4' -dimethylbiphenyl | 150/ 25 gm |
| Cyano-naphthalene | 68/ 25 mg |
| 9,9- dimethyl-9H-fluorene | 112/ 1 gm |
| Biphenyl | 17/ 25 gm |
| Naphthalene | 16/ 25 gm |
| 2-methylnaphthalene | 23/ 25 gm |
| 1-methylnaphthalene | 18/ 25 gm |

* according to <https://www.fishersci.com/us/en/home.html>

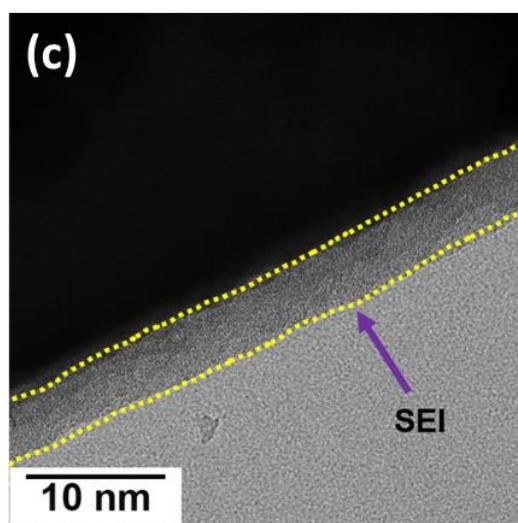
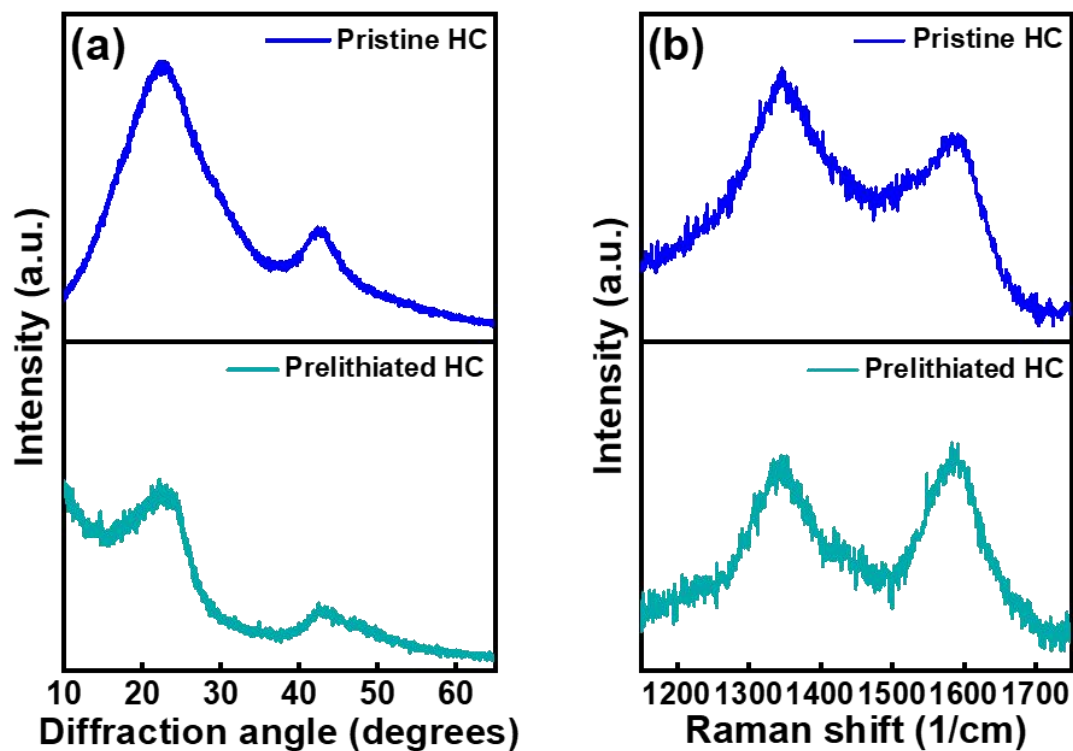


Figure S1. (a) X-ray diffraction patterns and (b) Raman spectra of pristine HC and HC prelithiated using Li-1-M-Naph/G1 solution. (c) TEM image of HC electrode prelithiated using Li-1-M-Naph/G1 solution.

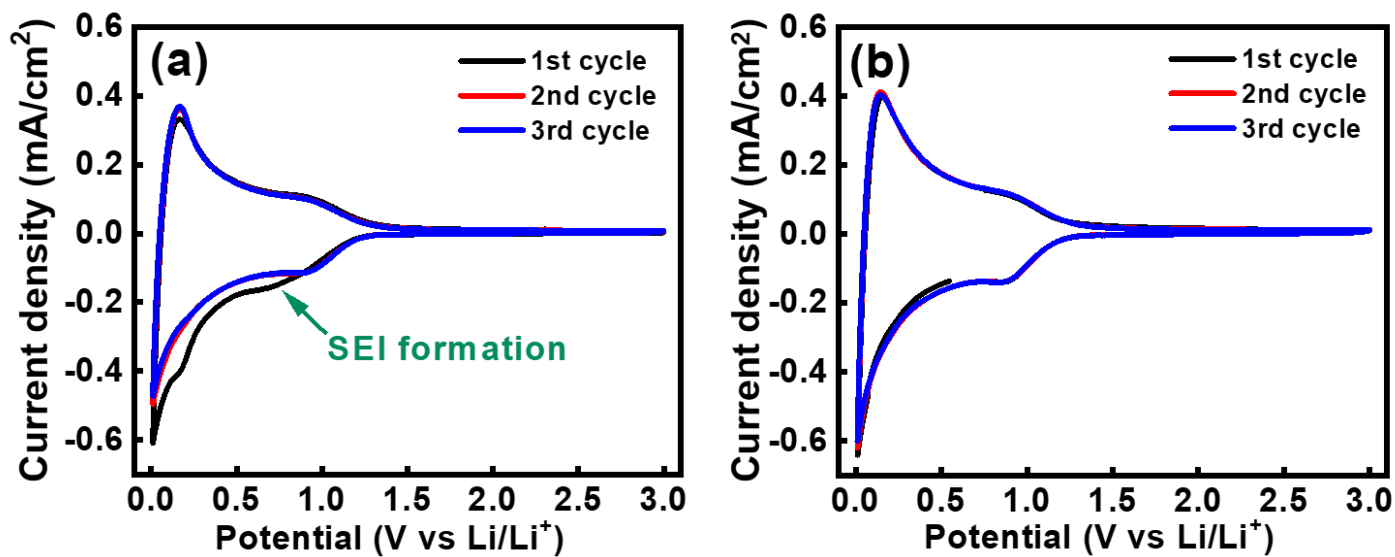


Figure S2. CV curves of (a) pristine and (b) Li-Naph/G1 HC electrode measured at potential scan rate of 0.2 mVs⁻¹.

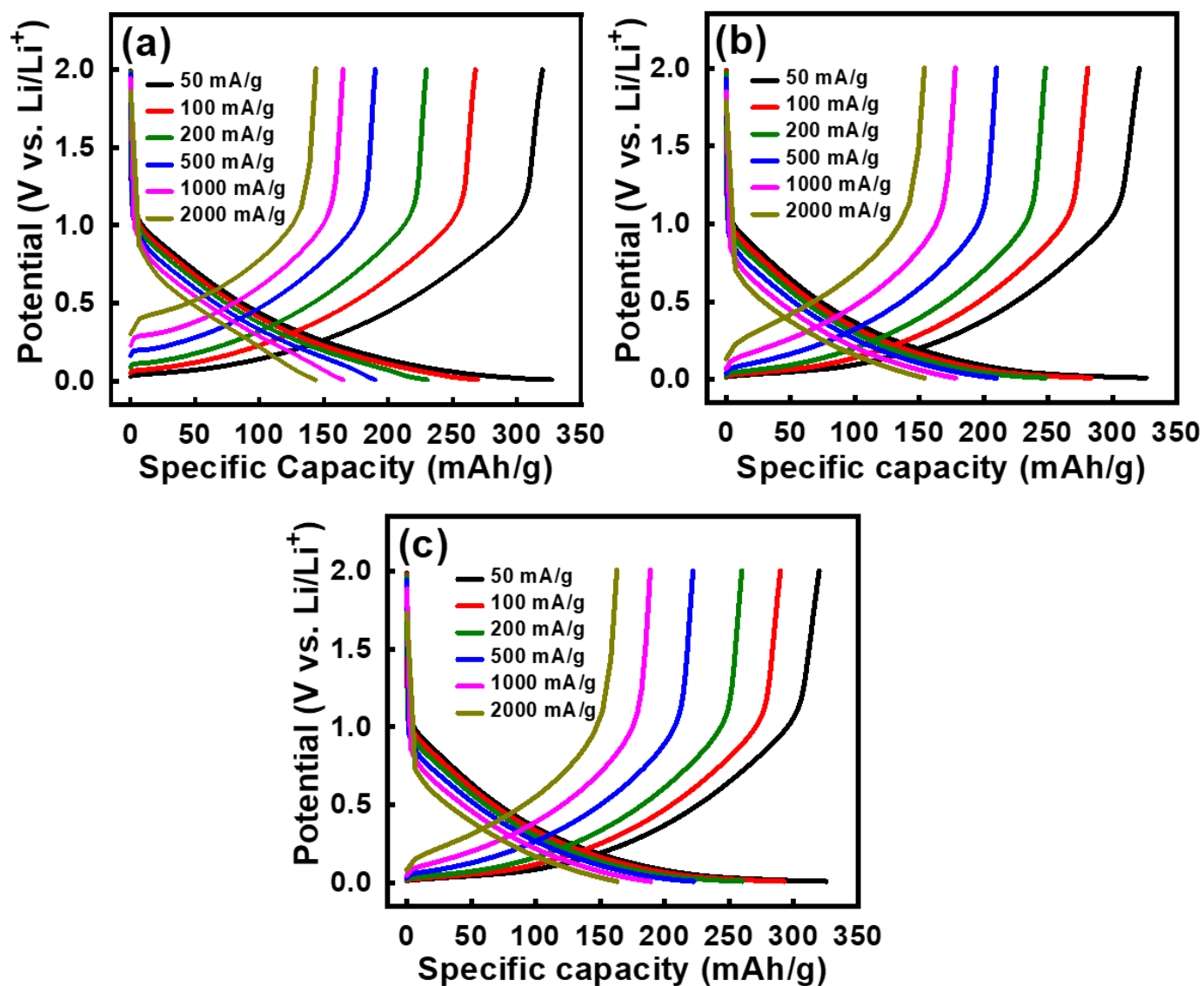


Figure S3. Charge-discharge curves of (a) pristine, (b) Li-Naph/G1, and (c) Li-2-M-Naph/G1 HC electrodes measured at various current rates.

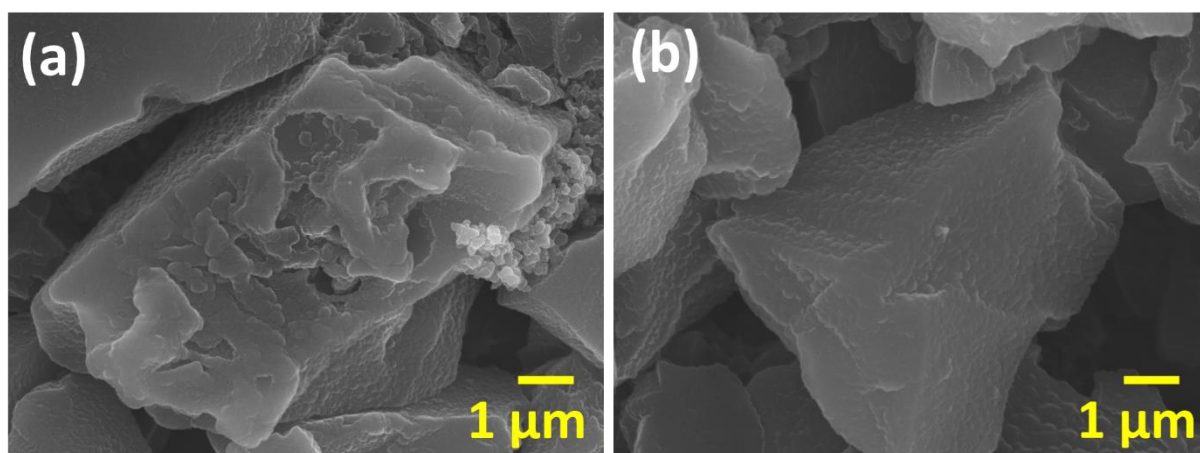


Figure S4. SEM images of (a) pristine and (b) Li-1-M-Naph/G1 HC electrodes after 500 charge-discharge cycles.

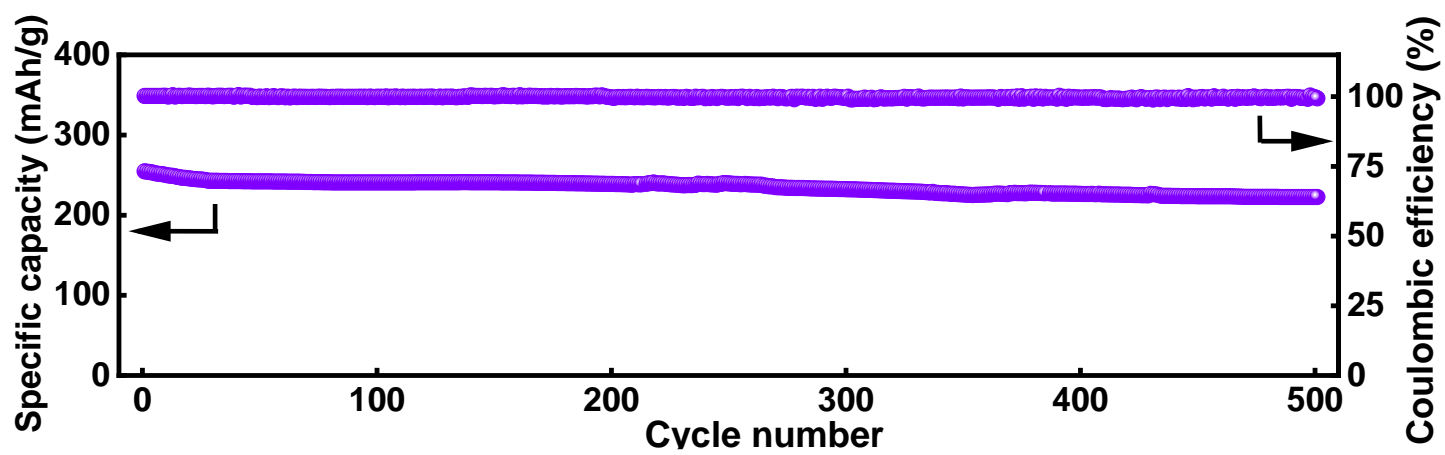


Figure S5. Cycling stability data of Li-1-M-Naph/G1 HC electrode measured at 400 mA g^{-1} for 500 cycles at $50 \text{ }^\circ\text{C}$.

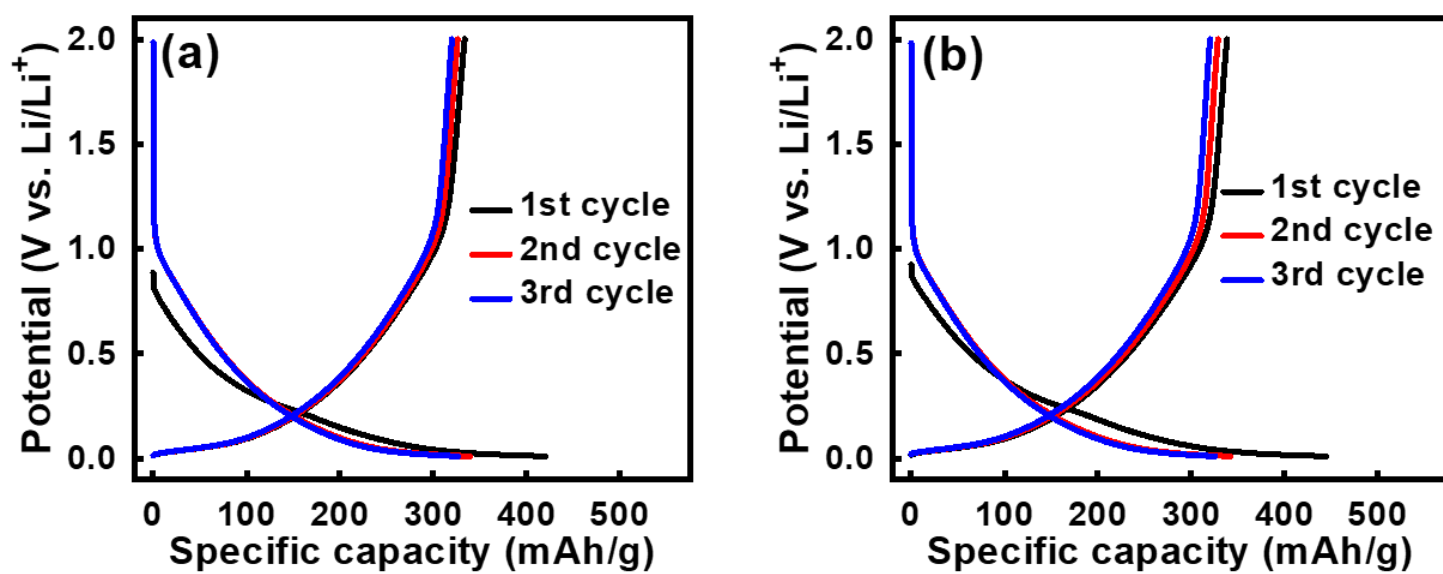


Figure S6. Initial charge-discharge curves of (a) Li-1-M-Naph/G2 and (b) Li-1-M-Naph/G3

HC electrodes measured at 50 mA g^{-1} .

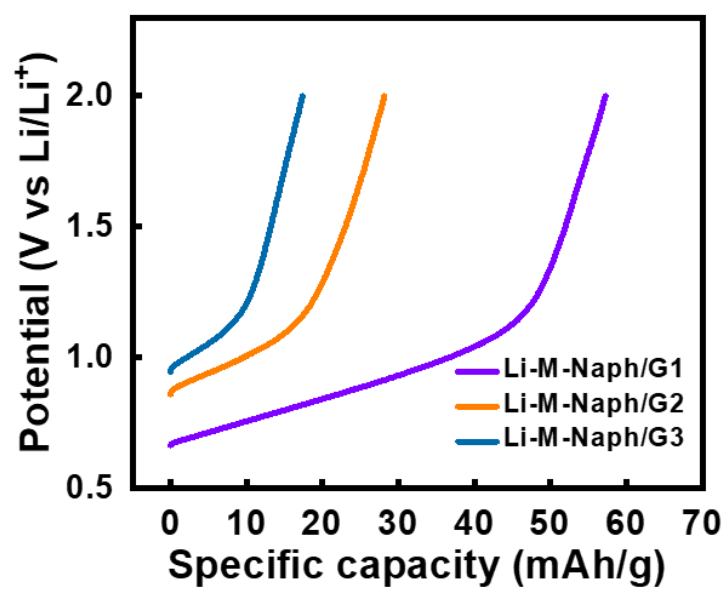


Figure S7. Direct-discharge curves of various prelithiated HC electrodes measured at 50 mA g⁻¹.

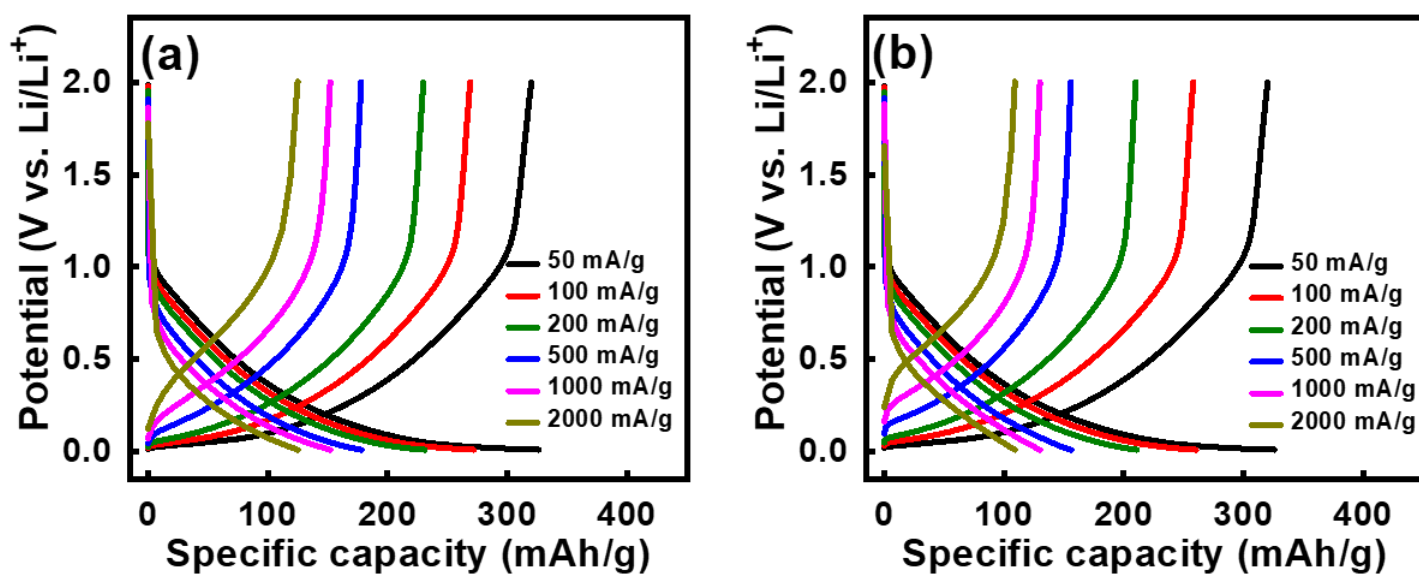


Figure S8. Charge-discharge curves of (a) Li-1-M-Naph/G2 HC and (b) Li-1-M-Naph/G3 HC electrodes measured at various current rates.

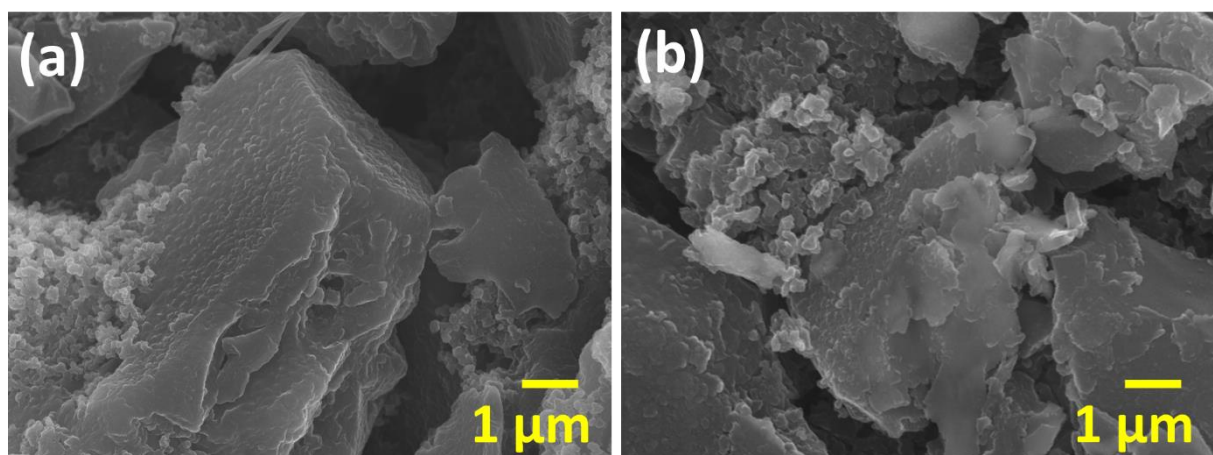


Figure S9. SEM images of (a) Li-1-M-Naph/G2 and (b) Li-1-M-Naph/G3 HC electrodes after 500 charge-discharge cycles.

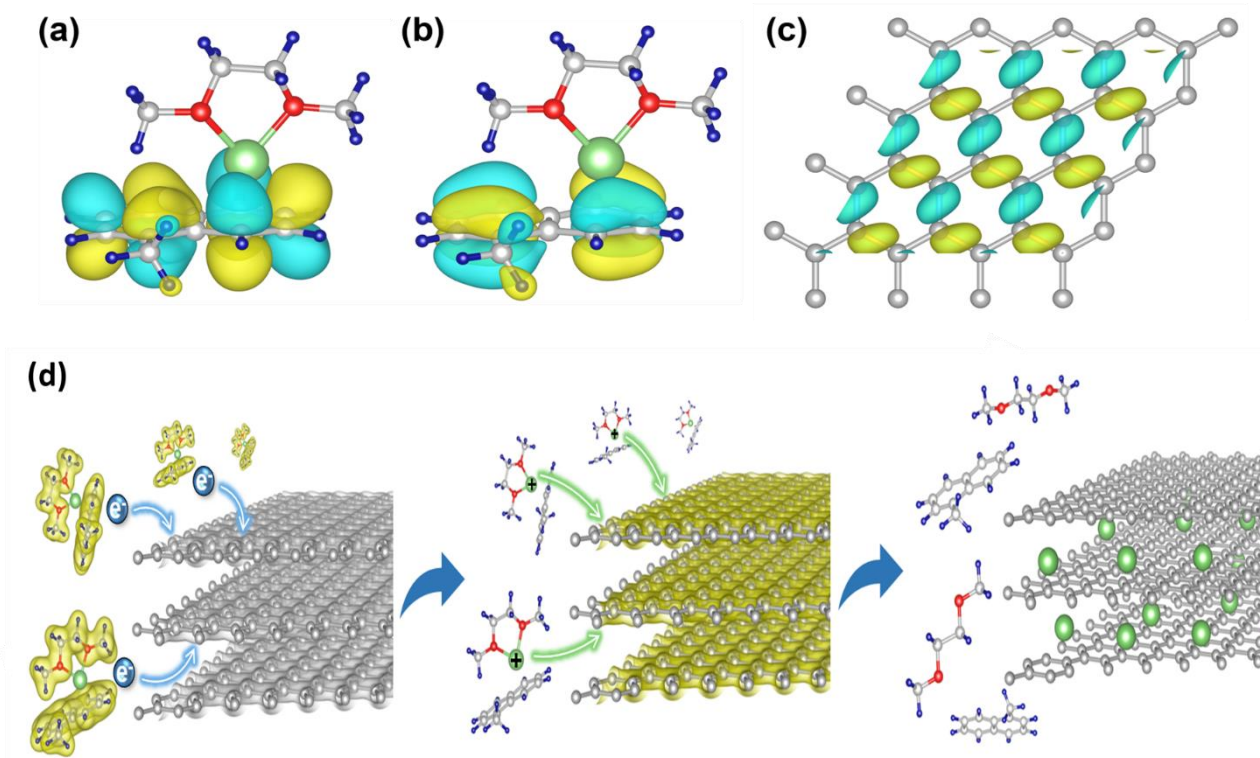


Figure S10. The wavefunction distribution of (a) α -HOMO of Li-1-M-Naph/G1, (b) β -HOMO of Li-1-M-Naph/G1, and (c) LUMO of graphene monolayer. (d) The proposed prelithiation mechanism. The yellow translucent area indicates the spatial distribution of electron charge within the molecules.

The lowest unoccupied molecular orbital (LUMO) energy levels for mono-layer, bi-layer, and tri-layer carbons are calculated to be -4.329 , -4.360 , and -4.351 eV, respectively (the vacuum level is aligned to 0 eV). By comparing these energy levels with those of the various Naph compounds (see **Figure 2(c)**), it is evident that the LUMO energy levels of the layered carbons are lower than the α -HOMO energy levels of LACs. Moreover, the wavefunction analysis shows a notable similarity in orbital symmetry between the frontier orbital of Li-1-M-Naph/G1 and a graphene layer, as shown in **Figure S10(a-c)**. Consequently, based on the frontier orbital theory,^[1,2] electrons from the Naph compound can effectively transfer to the carbon layer. Subsequently, the negatively charged HC triggers the desolvation of Li^+ ions in the LAC solution and drives the Li^+ insertion into the carbon layers, as schemed in **Figure S10(d)**.

Reference

1. K. Fukui, T. Yonezawa, H. Shingu, *J. Chem. Phys.* 1952, 20, 722.
2. K. Fukui, T. Yonezawa, C. Nagata, H. Shingu, *J. Chem. Phys.* 1954, 22, 1433.

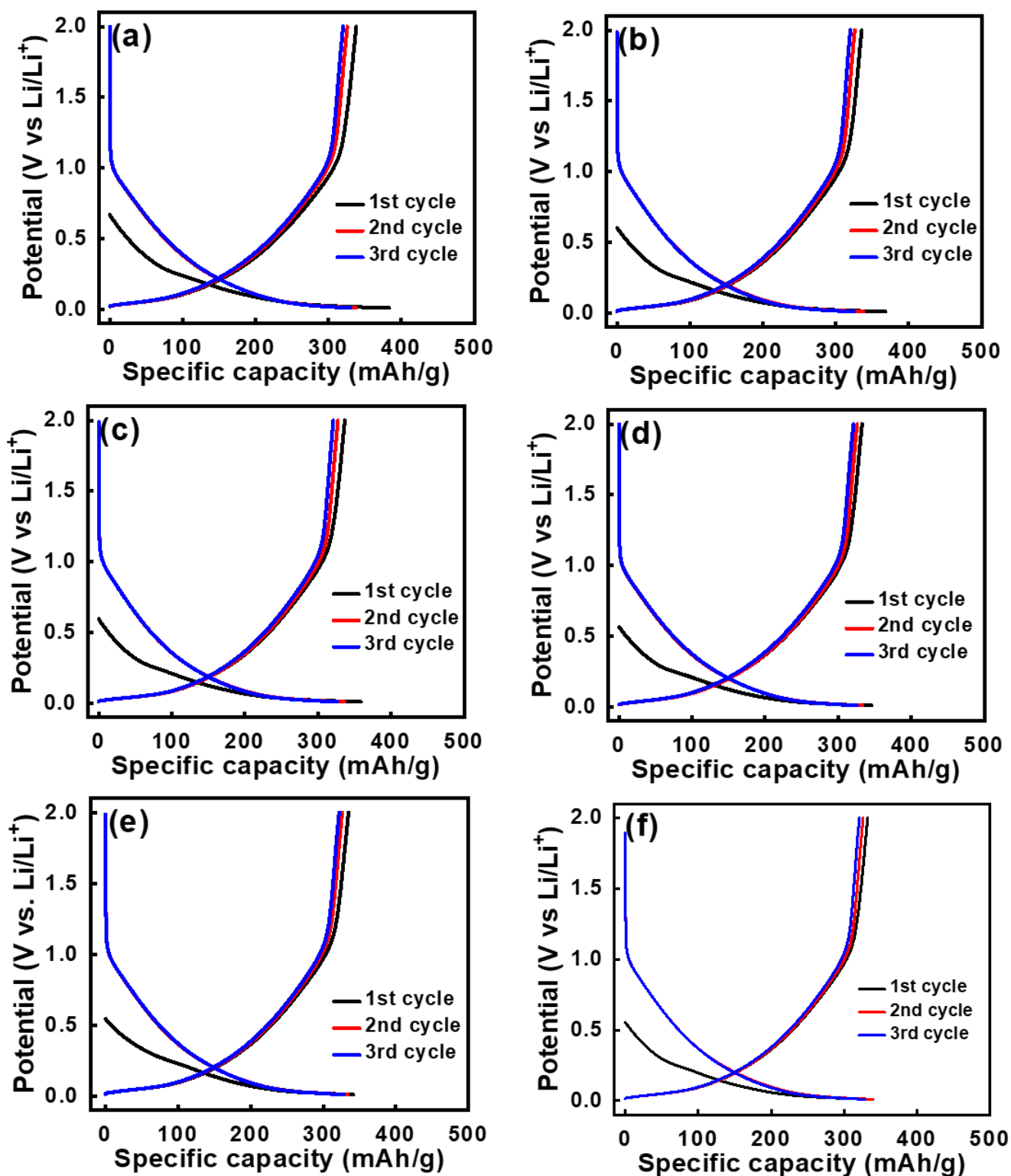


Figure S11. Initial charge-discharge curves (measured at 50 mA g⁻¹) of HC electrodes prelithiated using Li-1-M-Naph/G1 solution with aging times of (a) 2 h, (b) 4 h, (c) 6 h, (d) 8 h, (e) 10 h, and (f) 12 h.

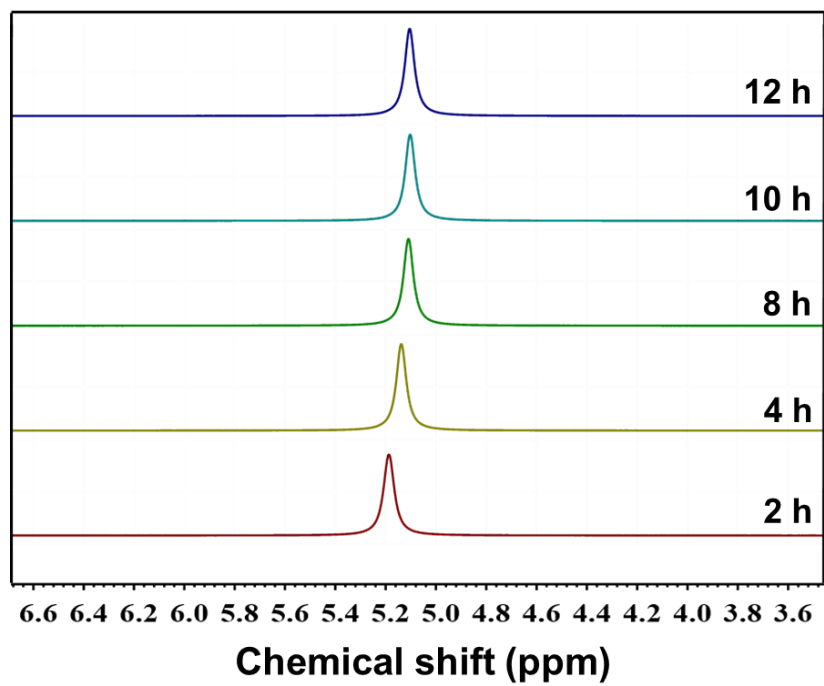


Figure S12. ^7Li NMR spectra of Li-1-M-Naph/G1 solution with various aging times.

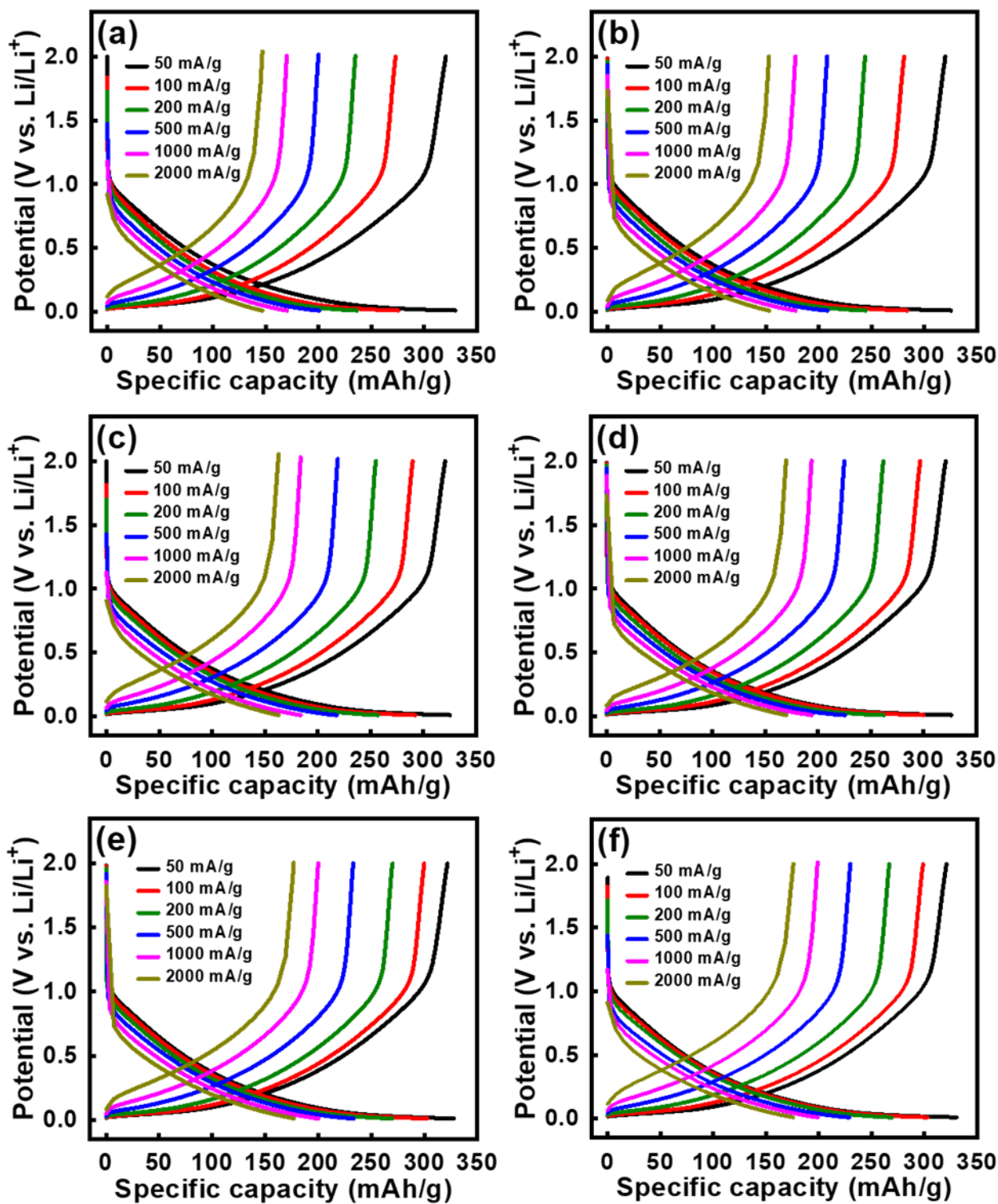


Figure S13. Charge-discharge curves (measured at various current rates) of HC electrodes prelithiated using Li-1-M-Naph/G1 solution with aging times of (a) 2 h, (b) 4 h, (c) 6 h, (d) 8 h, (e) 10 h, and (f) 12 h.

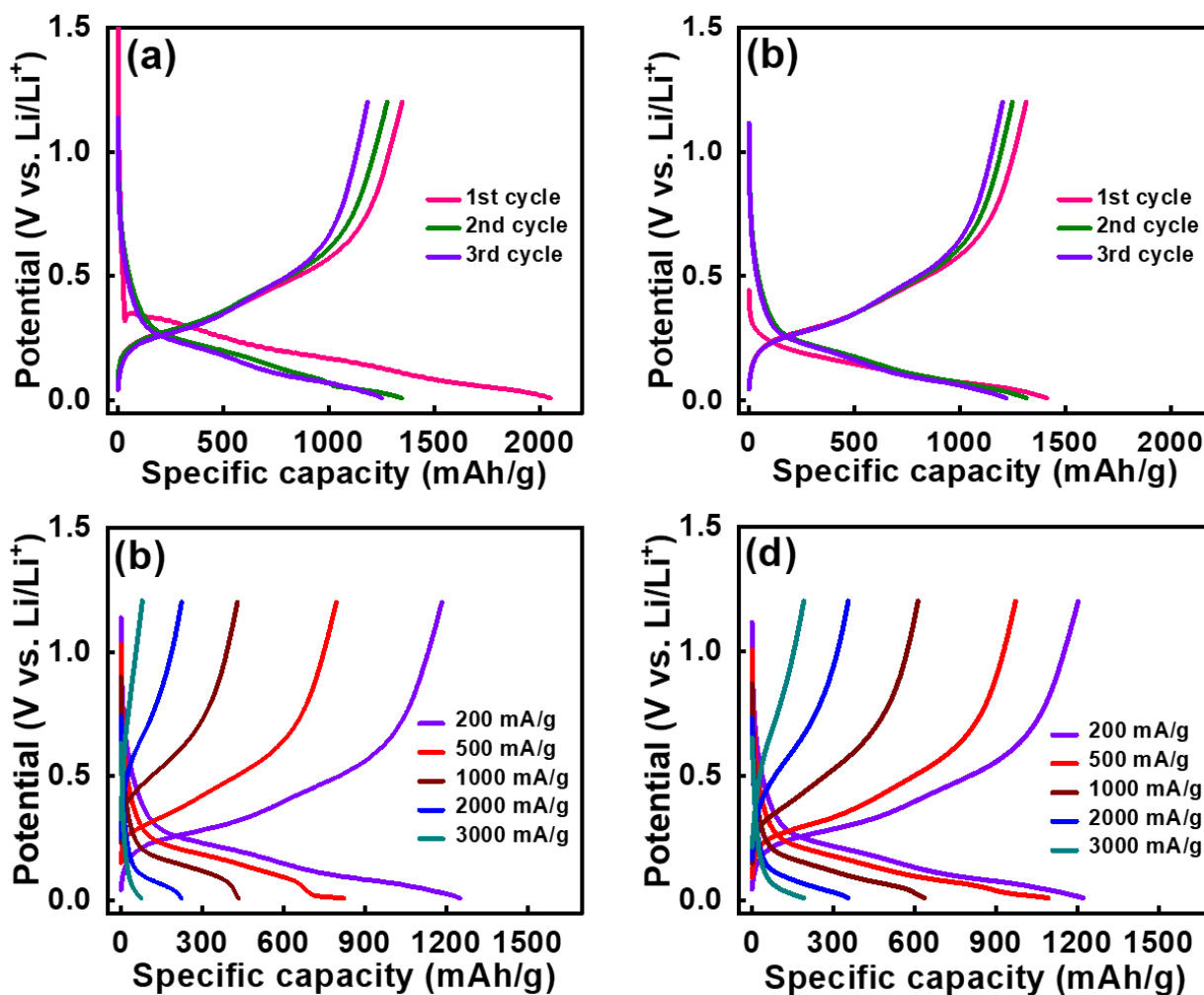


Figure S14. Initial charge-discharge curves measured at 200 mA g⁻¹ for (a) pristine SiO_x and (b) prelithiated SiO_x electrodes. Charge-discharge profiles measured at various rates for (c) pristine SiO_x and (d) prelithiated SiO_x electrodes. The Li-1-M-Naph/G1 solution was used for prelithiation.

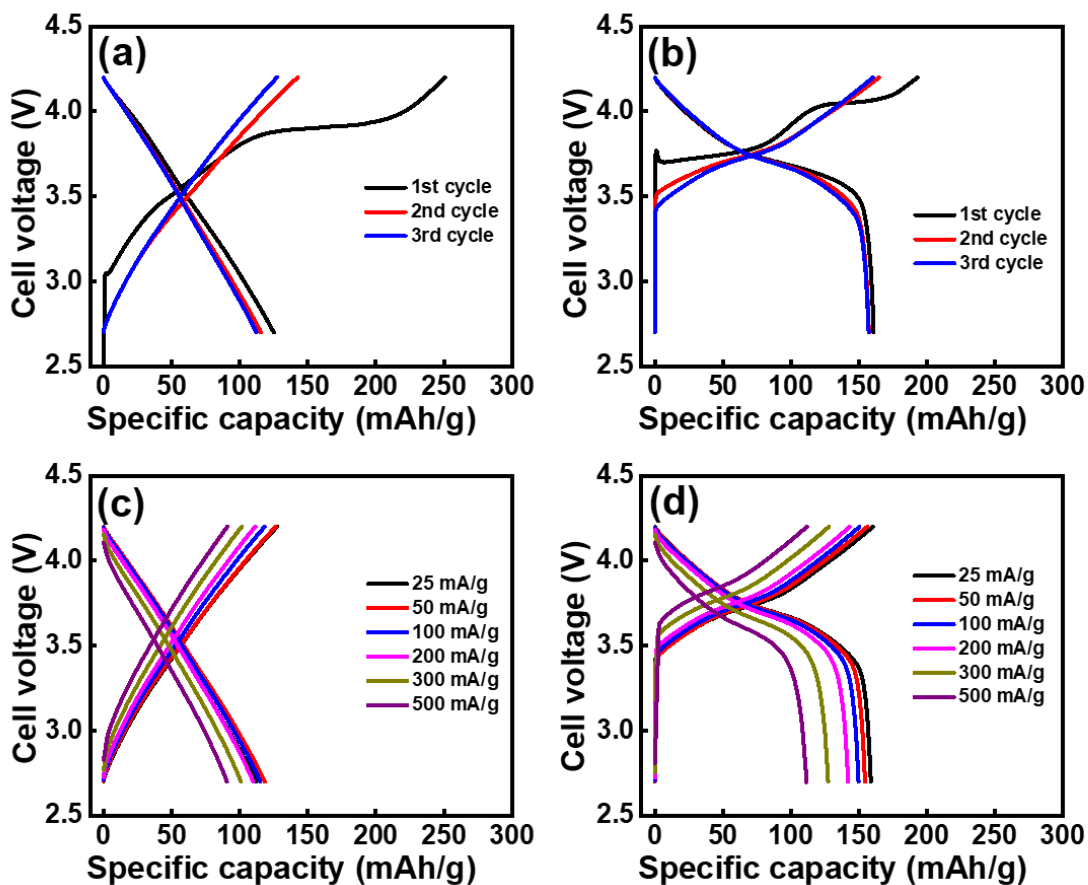


Figure S15. Initial charge-discharge curves measured at 25 mA g^{-1} (based on $\text{LiNi}_{0.6}\text{Co}_{0.2}\text{Mn}_{0.2}\text{O}_2$) for (a) pristine $\text{HC}||\text{LiNi}_{0.6}\text{Co}_{0.2}\text{Mn}_{0.2}\text{O}_2$ and (b) prelithiated $\text{HC}||\text{LiNi}_{0.6}\text{Co}_{0.2}\text{Mn}_{0.2}\text{O}_2$ full cells. Charge-discharge profiles measured at various rates for (c) pristine $\text{HC}||\text{LiNi}_{0.6}\text{Co}_{0.2}\text{Mn}_{0.2}\text{O}_2$ and (d) prelithiated $\text{HC}||\text{LiNi}_{0.6}\text{Co}_{0.2}\text{Mn}_{0.2}\text{O}_2$ full cells. The Li-1-M-Naph/G1 solution was used for prelithiation.